Published in final edited form as:
Mol Cell Neurosci. 2012 July ; 50(3-4): 238–249. doi:10.1016/j.mcn.2012.05.007.

IgSF8: a developmentally and functionally regulated cell adhesion molecule in olfactory sensory neuron axons and synapses

Arundhati Ray[*] and **Helen B. Treloar**[*,†]

[*]Department of Neurosurgery, Yale University School of Medicine, 333 Cedar Street, New Haven, CT 06520-8082, USA, arundhati.ray@yale.edu

Abstract

Here, we investigated an Immunoglobulin (Ig) superfamily protein IgSF8 which is abundantly expressed in olfactory sensory neuron (OSN) axons and their developing synapses. We demonstrate that expression of IgSF8 within synaptic neuropil is transitory, limited to the period of glomerular formation. Glomerular expression decreases after synaptic maturation and compartmental glomerular organization is achieved, although expression is maintained at high levels within the olfactory nerve layer (ONL). Immunoprecipitations indicate that IgSF8 interacts with tetraspanin CD9 in the olfactory bulb (OB). CD9 is a component of tetraspanin-enriched microdomains (TEMs), specialized microdomains of the plasma membrane known to regulate cell morphology, motility, invasion, fusion and signaling, in both the nervous and immune systems, as well as in tumors. *In vitro*, both IgSF8 and CD9 localize to puncta within axons and growth cones of OSNs, consistent with TEM localization. When the olfactory epithelium (OE) was lesioned, forcing OSN regeneration *en masse,* IgSF8 was once again able to be detected in OSN axons terminals as synapses were reestablished. Finally, we halted synaptic maturation within glomeruli by unilaterally blocking functional activity and found that IgSF8 did not undergo exclusion from this subcellular compartment and instead continued to be detected in adult glomeruli. These data support the hypothesis that IgSF8 facilitates OSN synapse formation.

Keywords

development; glomeruli; olfactory sensory neuron; synaptosomes; tetraspanin; tetraspanin-enriched microdomain

1. INTRODUCTION

The coding of olfactory information is crucial for olfactory function, and underlies behaviors such as feeding, mating, aggression and predation. Unlike other sensory systems which employ point-to-point mapping of their receptive fields onto cortical targets, olfactory

[*]Author to whom correspondence should be addressed: Helen B Treloar, Ph.D., Department of Biology, Wesleyan University, 52 Lawn Avenue, Middletown, CT 06459, Telephone - 860.685.2403, htreloar@wesleyan.edu.
[†]Department of Biology (Neuroscience and Behavior) Wesleyan, University, 52 Lawn Avenue, Middletown, CT 06459 (present address), htreloar@wesleyan.edu

projections display a convergent topography from the olfactory epithelium (OE) to the olfactory bulb (OB). It is well established that each olfactory sensory neuron (OSN) in the epithelium expresses a single odorant receptor (OR) and all OSNs expressing the same OR target stereotypic glomeruli in the OB (Mombaerts, 2006).

The development of this pathway is precocious, and is necessary for sensory function. In a screen of candidate neurogenic and stem cell genes in developing olfactory sensory neurons, we found high expression of IgSF8, a member of the Ig super family. In the immune system and carcinoma cells, IgSF8 regulates cell motility and polarity via interactions with both direct binding partners (tetraspanins) and indirect partners present within tetraspanin (Tspan) webs (Yanez-Mo et al., 2009). The function of IgSF8 in the nervous system, however, is unknown. Cell adhesion molecules (CAMs) that belong to the Ig superfamily (IgSF) have documented roles in axon outgrowth and navigation (Maness and Schachner, 2007; Plachez and Richards, 2005). In the olfactory system Ig-containing CAMs such as neural cell adhesion molecule (NCAM), olfactory cell adhesion molecule (OCAM) and L1 have been implicated in regulating olfactory development (Miragall et al., 1989; Treloar et al., 1997; Yoshihara et al., 1997). Therefore we selected IgSF8 for further study to test the hypothesis that it has a role in the development of the olfactory pathway.

Here, we characterize IgSF8 expression during the formation of glomeruli, as the OSN axons arrive at the OB. Consistent with a role in OSN development, we describe the differential distribution of IgSF8 along OSN axons and enrichment in newly formed glomeruli. IgSF8 is initially highly expressed in axon terminals, but is down-regulated in adult glomeruli after synapses have been established. When OSN replacement is induced by a chemical lesion, IgSF8 is re-expressed in axon termini. Moreover, expression of IgSF8 is maintained at high levels at later stages of development if functional activity is blocked with unilateral naris occlusions. Furthermore, we demonstrate that IgSF8 interacts with the Tspan CD9 and is present in OB synaptosomes, consistent with the hypothesis that IgSF8 is present in Tspan-enriched microdomains (TEMs) in OSNs. Collectively, these data suggest that IgSF8 has a role in OSN maturation and synaptogenesis.

METHODS

2.1 Animals

2.1.1 RNA/protein analysis—Pregnant, time-mated CD-1 mice (Charles-River, Wilmington, MA) were euthanized with CO_2. Embryos (n = 9 - 12 at each age) were collected by cesarean section on gestational days 13, 15, and 17 (day of positive vaginal plug was designated day 0) and immediately decapitated. Early postnatal mice at postnatal day (P) 2 (n = 9) were rapidly decapitated. Older postnatal mice (P7 and P14) and adult mice (n = 3 - 6 at each age) were euthanized with CO_2. Olfactory bulbs (OBs) and epithelium (OEs) were dissected and immediately frozen in dry ice.

2.1.2 Tissue sections—Embryos were collected by cesarean section from pregnant, time-mated CD-1 mice (Charles River Laboratories, MA) at embryonic day (E)13, E15 and E17 and postnatal (P)2 mice were rapidly decapitated. Heads were immersion fixed in 4% paraformaldehyde (PFA) in PBS at 4°C overnight. Mice at P7, P14, P21 and adults were anesthetized with sodium pentobarbital (80 mg/kg, i.p.; Nembutal; Abbott laboratories, Chicago, IL) and perfused with cold 4% PFA in PBS, pH 7.4. Brains were removed and postfixed for 2 hrs at 4°C in the perfusate. Following fixation, tissue was washed in PBS for at least 2 hrs. Tissue was then either cryoprotected, frozen and prepared for cryosectioning as previously described (Treloar et al., 2009) or embedded in agarose and coronally sectioned (50μm) using a vibratome.

Animal protocols were reviewed and approved by the Yale Animal Care and Use Committee (IACUC approval #10956).

2.2 Targeted Microarrays

2.2.1 RNA extraction—RNA was extracted using RNeasy Plus Mini kit (Qiagen, Valencia, CA) following manufactures instructions. Briefly, 20 - 30μg of frozen OB tissue was homogenized in Buffer RLT Plus with β-mercaptoethanol. DNA was removed through gDNA Eliminator column, and extracts were washed with 70% ethanol in RNeasy spin column. After several washes with Buffer RW1 and Buffer RPE, RNA was eluted with water. Total RNA concentrations were determined using a spectrophotometer.

2.2.2 cRNA synthesis and OligoGEArray Hybridization—cRNA was synthesized from OB cDNA, and biotin-labeled using the TrueLabeling-AMP™ 2.0 Kit (SuperArray Biosciences, MD). The membranes were hybridized overnight with 2μg of biotin-labeled cRNA probe. They were washed and developed according to manufacturer's instructions (SuperArray Biosciences, MD). Images were captured with a Kodak Gel Logic 440 Image Station. Genes present on array are detailed in Supp. Data Table 1.

2.2.3 Data Analyses—Images were analyzed using ImageJ (Rasband, W.S., Image J, U. S. National Institutes of Health, Bethesda, Maryland, USA http://rsb.info.nih.gov/ij/, 1997-2009. Briefly, spot intensity of genes of interest (GOI) was determined using a standard region of interest (ROI) and then normalized relative to GAPDH expression (100%) and a blank (0%). Data is expressed as a % of GAPDH expression.

2.3 In situ hybridization

2.3.1 Riboprobe preparation—Antisense and sense probes were generated from a plasmid containing the complete coding region of IgSF8 obtained from ATCC (clone number 10470463; Manassas, VA). Probes were synthesized using *in vitro* transcription MEGAscript kit (Ambion, Austin, TX), incorporating 1μl of digoxigenin-11-UTP (Roche Diagnostics, Indianapolis, IN) into the provided protocol.

2.3.2 Hybridization—Protocol was followed as described in Akins et al., 2007. Probe was diluted 1ng/μl in hybridization buffer and incubated at 65°C. Signal was visualized using NBT/BCIP (Roche) for 2 hours and mounted with Crystal/Mount mounting medium (Biomeda). Digital images were collected using an Olympus Magnafire camera attached to an Olympus BX51 microscope.

2.4 Immunohistochemistry

Immunostaining was performed as previously described (Treloar et al., 2009). Primary antibodies: goat anti-IgSF8 (1:1000; R&D Systems, Minneapolis, MN.); rat anti-NCAM (1:1000; Millipore, Billerica, MA); rabbit anti-NCAM (1:1000; Millipore); rat anti-CD9 (1:500; BD Pharmingen, San Jose, California); rabbit anti-VGluT2 (1:2000; Synaptic Systems, Goettingen, Germany); rabbit anti-VGluT1 (1:2000; Synaptic Systems); rabbit anti-GAP43 (1:1000; Novus, Littleton, CO) rabbit anti-TH (1:1000; Millipore). The goat anti-IgSF8 and rat anti-CD9 antibodies have been characterized by Glazar and Evans, 2009.

Analyses—Fluorescent images were semi-quantitatively analyzed via line scan using ImageJ. Briefly, line scans were taken across the olfactory nerve layer and relative optical density was determined for NCAM, VGluT2 and IgSF8. Data from all three markers was plotted on a graph to assess relative distributions.

2.5 Immunoblotting and Deglycosylation

2.5.1 Protein extraction and immunoblotting—Mice OBs from different ages were homogenized in lysis buffer (20mM Tris-HCl pH7.4, with protease inhibitor cocktail (Roche) using a dounce homogenizer. The homogenates were sonicated for 5min, centrifuged at 800*g* for 5min at 4°C and supernatants were collected for protein estimation using Pierce BCA Protein Assay kit (Thermo Fisher Scientific). 10μg of each protein sample was run on a NuPAGE Novex 4-12% Bis-Tris gel (Invitrogen). Resolved protein bands were transferred to a nitro-cellulose membrane using iBlot dry blotting system (Invitrogen) for 7mins. The membrane was blocked with 5% milk prepared in TBS-Tw (Tris buffered saline pH7.4, 0.3 %Tween) for 30 mins, incubated with primary antibody for 60min. The following primary antibodies were diluted in blocking solution: goat anti-IgSF8 (1:5000; R&D); mouse anti-β-actin (1:5000; Abcam, Cambridge, MA); rat anti-CD9 (1:1000; BD Pharmingen); mouse IgM anti-Synaptophysin (1:5000; Millipore) and then washed in TBS-Tw 3 × 15min. The blot was incubated with an appropriate HRP-conjugated secondary antibody raised in donkey (Jackson ImmunoResearch, West Grove, PA) diluted 1:10000 for 60min, washed in TBS-Tw 3 × 10min and detected using ECL Western blotting reagents (GE Healthcare, Piscataway, NJ). Blots were stripped with Restore Western Blot stripping buffer (Thermo Fisher Scientific, Waltham MA) for 5min, washed with TBS-Tw up to three times and re-probed with another primary antibody. Molecular weight of protein bands was determined using Carestream Molecular Imaging software and molecular weight markers (Precision Plus Protein Dual Color standards, Bio-Rad; Novex Sharp Pre-Stained Protein standards, Invitrogen; MagicMark XP Western standard, Invitrogen).

2.5.2 Deglycosylation—For glycosylation analyses, OB homogenates were treated with PNGaseF (N-glycosidase F; New England Biolabs, Beverly, MA) according to manufacturer's instructions, and were characterized by immunoblotting.

2.6 Immunoprecipitation

P2 OBs were dissected and homogenized in cold lysis buffer (20mM Tris-HCl pH7.4, 1mM EDTA, 150mM NaCl, 1%Brij 96, 0.02% NaN_3, protease inhibitor cocktail (Roche)). OB homogenate was incubated with 10 μg of antibody (rat anti-CD9, BD-Pharmingen; goat anti-IgSF8, R&D) for 60min at 4°C with constant rocking. 50μl of PureProteome Protein G magnetic beads (Millipore) were washed three times with lysis buffer as per manufacturer's instructions and added to the antigen-antibody complex. This complex was incubated for 10 min at room temperature (RT) and then rinsed three times with lysis buffer. The immune complex was eluted by boiling in LDS buffer (Invitrogen) and run on a NuPAGE Novex 4-12% Bis-Tris gel (Invitrogen). Protein bands were characterized by immunoblotting.

2.7 OB fractionation and synaptosome isolation

OBs from P7 litter were homogenized using a dounce homogenizer at 100g in cold synaptosome buffer (0.32M sucrose, 10mM Hepes pH 7.4 (American Bioanalytical, MA), protease inhibitor cocktail (Roche)) and centrifuged at 600g for 10min at 2°C to remove nuclear material. The postnuclear supernatant (S_1) was further centrifuged at 7500g for 15min at 2°C to obtain synaptosomal supernatant (S_2) and crude synaptosomal pellet (P_2). The P_2 pellet was resuspended in synaptosome buffer. 1μg of the P_2 fraction was run on a Bis-Tris gel and characterized by immunoblotting.

2.8 Unilateral Naris Occulsion

CD1 pups (postnatal day 2) were anesthesized by immersion in an icebath, protected with a surgical glove. The left naris was cauterized using a brief electrocautery pulse and immediately after, treated with a topical antibiotic-pain relieving cream (Neosporin). The

cauterized pups were warmed to RT and then returned to their mother. Mice were transcardially perfused two months after naris occlusion, and the OBs were dissected and sectioned. Activity-dependent expression of IgSF8 was established by comparing the occluded OB with the contralateral contol OB. The efficiency of occlusion was demonstrated by the down-regulation of tyrosine hydroxylase protein in the glomeruli of the occluded OB compared to the contralateral OB (Gomez et al., 2007).

2.9 Epithelial ablation

Ablation of the olfactory epithelium was achieved using the methimazole administration paradigm described by (Booker-Dwyer et al., 2008). Briefly, adult mice (>60 days) were intraperitoneally injected with methimazole (Sigma) in sterile saline (50μg/g of body weight) on the first and third days of treatment. Mice injected with saline served as sham controls. Mice were transcardially perfused after one week and four weeks of injection. The OBs from these animals were sectioned using a vibratome to obtain 75μm coronal sections which were immunostained to analyze for OSN regeneration.

2.10 Tissue culture

Explant cultures were prepared as previously described (Treloar et al., 2009). Explants were grown on poly-D-lysine (PDL, Sigma; 50μg/ml) and laminin (20μg/ml, Invitrogen) coated 8-well Culture Well chambered coverglass (Grace Biolabs). Explants were cultured for 5 days at 37°C + 5% CO_2 before being fixed in 4% PFA/4% sucrose in PBS for 30 min at RT followed by 3 rinses in PBS. *Immunostaining:* Cultures were immunostained as previously described (Treloar et al., 2009), with the omission of a detergent, using a rabbit anti-NCAM antibody (Millipore), a goat anti-IgSF8 antibody and a rat anti-CD9 antibody (BD). Staining was visualized using an Olympus BX51 fluorescence microscope and a 100X oil immersion objective.

2. RESULTS

3.1 Identification of IgSF8 in OE screening

During a targeted microarray screen (OMM-404; SABiosciences, Fredrick MD) of candidate neurogenic and stem cell genes in the developing olfactory epithelium (OE), we selected IgSF8, a member of the Ig superfamily for further study (Figure 1, and Table 1). These arrays identified several known developmentally regulated genes in the OE such as Fmr1, Lhx2, Npn1, Nlgn1, and Nogo (Figure 1A) and a number of candidate genes (e.g. IgSF8, Jag1 and Pcdhb16; Figure 1A). A factor in our selection of IgSF8 was the observation that CD9, a known binding partner of IgSF8 was also present in the OE (Figure 1A). In immune and tumor cells CD9 and IgSF8 modulate integrin-dependent cell motility and/or spreading. A primary reason that we focused our analyses on IgSF8 is the well established roles other members of the Ig superfamily play in olfactory pathway development. For example, OSNs express the cell adhesion molecules NCAM and N-cadherin which are important for olfactory pathway formation (Akins and Greer, 2006; Treloar et al., 1997). Similarly, they express many cell surface receptors which are members of the Ig superfamily, such as DCC, Neuropilin-1, DSCAM and Robos1-2 (Agarwala et al., 2001; Astic et al., 2002; Cho et al., 2007; Nagao et al., 2000).

3.2 IgSF8 mRNA expression in the developing olfactory system

Structurally, IgSF8 possesses a short signal sequence at the N terminus, four Ig-like domains, 3 putative N-glycosylation sites, a transmembrane domain and a short intracellular region (Yamada et al., 2006; Zhang et al., 2003) (Figure 2A). Limited data exists about the role of IgSF8 in the nervous system. During embryogenesis, IgSF8 mRNA has been

reported in the developing nervous system including the OE (Murdoch et al., 2003) and in a tissue wide northern screen highest expression was detected in whole human brain (Bonkobara et al., 2003). IgSF8 induces neurite outgrowth of Neuro-2a cells *in vitro* and therefore has a proposed role in the regulation and maintenance of neurite outgrowth (Yamada et al., 2006). In light of these previous reports, we hypothesized that IgSF8 may have a role in the regulation of OSN axon outgrowth and synaptogenesis. To test this hypothesis, we performed a series of experiments to characterize IgSF8 expression and function in the developing olfactory sensory neurons.

Using a riboprobe against the full length coding sequence, we performed *in situ* hybridization (ISH) to localize IgSF8 mRNA expressing cells in both the OE and OB at postnatal day 2 (P2). The ISH signal is widespread in the OE, vomeronasal organ and OB (Figure 2B-G). In both the OE (Figure 2D) and VNO (Figure 2F) IgSF8 mRNA expression is confined to sensory neurons (arrows), sustentacular cells (arrowheads) are free of IgSF8 expression. In the OB, IgSF8 mRNA is abundant in mitral cells (arrows, Figure 2G) and in a few scattered cells in the external plexiform layer (arrowheads) which are likely tufted cells. Staining is absent in the ONL (Figure 2C, G). Weaker signal is detected in the granule and periglomerular cells. No signal is observed in sections stained with sense riboprobe (Fig. 2E,H). These *in situ* data confirm the micro-array data, indicating that IgSF8 mRNA is expressed in the developing OE and OB.

3.3 IgSF8 protein expression in the developing olfactory system

To characterize IgSF8 protein expression during olfactory pathway formation, we performed immunolocalization experiments in coronal cryosections. At P2, IgSF8 was expressed in OSNs in a subcompartmental fashion. Staining was not present in OSN cell bodies (open arrowheads Figure. $3B_1$-B_3) or in the proximal segment of the axon (arrowheads Figure. $3B_1$-B_3), but was detected as axons entered larger fascicles (arrows Figure. $3B_1$-B_3); staining intensified across the olfactory nerve layer and was most intense in the glomeruli (Figure $3A_1$-A_3). This pattern suggests differential expression along the length of the axon, with the most intense expression at the terminal or distal segment at this age.

To characterize the temporal expression of IgSF8 protein we first performed western analyses using an IgSF8 polyclonal antibody and protein isolated from the OB at E15, E17, P0, P2, P4, P7, P14, P21 and adult (Figure. 4A). A band of ~75 kDa is detected at all ages although protein levels increase from E15 to P21. IgSF8 has a predicted Mr of 65kDa which suggests that the protein is glycosylated in the OB. Two faint bands were also observed at ~65kDa and ~55kDa in some samples. The ~65kDa band likely represents an unglycosylated form, and the lower band may represent a 50kDa cleaved fragment reported by Stipp et al., (2001a).

To confirm that IgSF8 is glycosylated, OB lysates were digested with PNGaseF to remove the N-linked carbohydrates. Upon enzymatic digestion, a 10kDa shift in the molecular size was observed (Figure 4B). The lysates treated with the enzyme had a molecular weight of 65 kDa, ~10 kDa lower than the untreated ones (Figure 4B) confirming that IgSF8 is N-glycosylated.

As IgSF8 showed temporal changes in expression on the Western, and to determine whether the differential subcellular distribution seen at P2 was stable throughout development, we performed immunolocalization analyses at a variety of developmental stages spanning the period of synaptogenesis (Kim and Greer, 2000). Specifically, we examined IgSF8 expression at E15, E17, P2, P7, P14 and adult (Figure 5). Using NCAM as a marker of all OSNs (Miragall et al., 1989) and the vesicular glutamate transporter 2 (VGluT2) (Gabellec

et al., 2007; Nakamura et al., 2005) as a synaptic marker, we documented IgSF8 expression in OSN axons during glomerular synaptogenesis.

At E15, when axons first exit the ONL and grow deeper into the OB dendritic zone (DZ) (Shay et al., 2008; Treloar et al., 1999) we observed widespread IgSF8 expression in $NCAM^+$ OSN axons (Figure 5A1-A2). VGluT2 expression is restricted to the terminal segment of axons, where they have grown into the DZ (Figure 5A1; Supp. Figure 1A). We do not see coalescence of axons and VGluT2 to protoglomeruli until E17 (Figure 5B1) consistent with our earlier reports (Treloar et al., 1999). At E17 VGluT2 and NCAM expression is abundant in these structures (Figure 5B1), while IgSF8 is enriched in protoglomeruli as compared to the ONL, colocalizing with VGluT2 (Figure 5B1-B2; Supp. Figure 1B).

Glomeruli are first identifiable at birth (Treloar et al 1999). At P2 IgSF8 is enriched in glomeruli, as compared to expression in the ONL (Figure 5C1-C2; Supp. Figure 1C). This was observed in all animals examined (n=9). It was co-expressed with VGluT2 and NCAM (Fig. 5C1). As compartmental organization of axons and dendrites within glomeruli developed through the first 3 postnatal weeks (Kim and Greer 2000), IgSF8 expression remained high within glomeruli (Figure 5D1-E1; Supp. Figure 1D-E) but expression decreased markedly within adult glomeruli (Figure 5F1-F2; Supp. Figure 1F). While occasional glomeruli were observed which maintained weak expression, these appeared random and did not maintain any topography between animals. Moreover, IgSF8 appeared down regulated within the inner olfactory nerve layer (ONL_i), with high expression being maintained within the outer ONL (ONL_o) only (Figure 5F1-F2; Supp. Figure 1F). These data suggest that after synapses have formed and glomerular structure (i.e. compartmental organization) has fully developed, IgSF8 expression is downregulated within OSN axon terminals and distal axon segments and expression is maintained only within the central segment of the axon. Diagram 1 details the subcellular distribution of IgSF8 in OSNs from immature glomeruli (P2 with recently formed synapses) and mature glomeruli (adult with established synapses. The differential expression of IgSF8 in axon terminals and stable expression in axon shafts raises the possibility that it may have different roles in different segments of the axon.

3.4 IgSF8 interacts with CD9 in the olfactory bulb

IgSF8 has two known direct binding partners, CD9 and CD81, which are Tspan proteins that have reported roles in sperm-egg fusion, regulation of metastasis, cell motility, myoblast fusion, and nervous system development (Kelic et al., 2001; Le Naour et al., 2000; Stipp and Hemler, 2000; Tachibana and Hemler, 1999; Zoller, 2009). IgSF8 is a key interacting partner of the CD9/CD81 complex (Charrin et al., 2003; Clark et al., 2001; Stipp et al., 2001), and is believed to mediate some functions attributed to this complex. We performed a series of immunoprecipitation experiments to determine whether IgSF8 interacts with CD9 in the olfactory system. When CD9 antibodies were used to pull down interacting proteins from lysate prepared from P2 OB, IgSF8 was detected in the immunoprecipitated proteins (Figure 6A). Likewise when IgSF8 antibodies were used to immunoprecipitate interacting proteins, CD9 was identified (Figure 6C). These data indicate that IgSF8 and CD9 interact in the developing olfactory system.

CD9 has been reported in the nervous system and has been implicated in neurite outgrowth via its interaction with α6/β1 integrin and L1 (Schmidt et al., 1996), but CD9 expression has not been reported in the olfactory system. Immunohistochemical staining of CD9 revealed strong expression in the OB (Figure $6E_1$-E_3). At P2, CD9 expression is strong in the olfactory nerve and glomerular layers (Figure $6E_1$). Double-labeling of IgSF8 and CD9 demonstrate co-expression of these two proteins in the OSN axons (Figure $6E_2$). CD9

expression is down regulated in the glomeruli at P21 but the expression is high in ONL (Figure 6F1-F2). This is consistent with IgSF8 expression pattern where IgSF8 is downregulated in the glomeruli but is maintained in the ONL(Figure 6F2-F3). Co-immunoprecipitation of IgSF8 with CD9 and its co-localization with CD9 in OB suggests that IgSF8 may be a component of a TEM formed by CD9 in the OS, and this complex may be involved in the development of axon connections and/or synaptogenesis in the OB.

If CD9 and IgSF8 are present in microdomains within the membrane in so-called Tspan webs or TEMs (reviewed in (Hemler, 2005; Yanez-Mo et al., 2009), then we reasoned *in vitro* we should see a punctate expression pattern, representative of these TEMs. Indeed, Stipp et al., (2000) reported such a distribution for Tspans CD151 and CD81 in cultured NT2N cells. Consistent with this hypothesis, both IgSF8 and CD9 exhibit a punctuate distribution in NCAM+ cultured OSNs, and are found in both neurites and growth cones (Figure 6H). Interestingly, these molecules only partially overlap, suggesting TEMs may exist in OSNs with different molecular compositions.

3.5 IgSF8 is present in OSN axon terminals

OB glomeruli are synaptic neuropil where OSN axons synapse primarily onto the dendrites of mitral cells. Also, within glomeruli mitral cell dendrites form dendrodendritic synapses with dendrites of interneurons, the periglomerular cells. As described above, IgSF8 was found to be enriched within glomeruli during the period of synaptogenesis. This observation led us to hypothesize that IgSF8 may be present at the synapse. VGluT2 is selectively found in axodendritic synapses within glomeruli, while VGluT1 is selectively found within dendrodendritic synapses within glomeruli (Gabellec et al., 2007). As we found ISH signal for IgSF8 within mitral and tufted cells within the OB, the possibility existed that even though no IgSF8 protein was detected in the EPL, some protein may have been selectively trafficked to the apical dendrites and be found in dendrodendritic synapses. Therefore we performed double labeling experiments with both VGlutT1 and VGluT2 at P14, when compartmental organization of axodendritic and dendrodendritic synapses has emerged (Figure 7A-B). We found exclusive co-localization with VGluT2 (Figure $7A_2$), with no overlap with VGluT1 (Figure $7B_2$).

To unequivocally confirm IgSF8 is present within synaptic compartments, we performed a series of fractionation experiments to isolate synaptosomes from the OB. Synaptosomes are a preparation of isolated nerve terminals which retain the synaptic machinery needed for uptake storage and release of neurotransmitters (Dunkley et al., 2008). OB were collected at P7, and homogenized and fractionated to isolate crude synaptosomes (Figure 7C). The isolated fractions together with crude lysate were immunoblotted with IgSF8 and synaptophysin. Synaptophysin is a synaptic vesicle associated protein and is commonly used as a control to show its enrichment in the synaptosomal fraction (Fogel et al., 2007). While VGluT2 would have been a desirable choice to assay here, the protein aggregates upon boiling, and thus is not suitable for western analyses. As our preparation includes terminals from all layers of the OB, we confirmed the presence of OSN terminals by blotting with OMP and showed a concomitant increase in OMP and synaptophysin (syp) expression in the synaptoptosomal fraction indicating the successful isolation of axodendritic terminals (Figure 7C). IgSF8 is present in the postnuclear faction (S_1) which is further processed to obtain synaptosome (P_2) and synaptosomal supernatant (S_2) fractions. IgSF8 is present in P_2 fraction but not in S_2 (Figure 7C) indicating that IgSF8 protein is enriched in synaptic terminals. However, it remains to be determined via further fractionation whether it is present at the synaptic plasma membrane.

3.6 IgSF8 in the regenerating olfactory system

Thus far these data suggest a role for IgSF8 in the process of synaptogenesis; it is enriched in developing glomeruli, and is down regulated in OSN terminals once synaptic stability is achieved. We reasoned that if IgSF8 was required for synapse formation, perhaps we would see it re-expressed if the OSNs were forced to regenerate. To test this hypothesis, we lesioned the OE using the olfactotoxin methimazole (Sakamoto et al., 2007), forcing the coordinated regeneration of the olfactory system (Figure 8). One week after lesion, NCAM positive OSN axons were markedly decreased in the glomerular layer (Figure 8B, B_1), with the few remaining axons also staining with GAP-43 (Figure 8B, B_2), indicating that some reinnervation of the OB by OSNs was occurring. Faint IgSF8 expression was observed in the ONL_i and in reinnervating axons (arrows Figure 8B, B_3), whereas no IgSF8 was observed in the ONLi or glomerular layer of the saline injected animal (Figure 8A, A_3). At this timepoint, GAP-43+ OSNs have re-established contact with the OB (Schwob, 2002). Four weeks post lesion, NCAM+/GAP43+ OSN axons have reinnervated glomeruli (Figure 8C, $C_{1\text{-}2}$). While basic compartmental organization is re-established, the fine structure of interdigitating axons (NCAM+) and dendrites (NCAM-) is not restored to its previous complexity (c.f. Fig. 8C vs 5E). Glomeruli have a more rudimentary appearance with large, thick axonal compartments. IgSF8 was found to be re-expressed in these regenerated glomeruli, once again being expressed by OSNs in their distal axons and terminals (Figure $8C_3$).

3.7 IgSF8 expression is regulated by functional activity

As IgSF8 is downregulated in adult glomeruli, presumably after synapses are fully formed, we reasoned that activity might be important for this change in expression. To test this hypothesis we blocked functional activity in neonatal animals, via unilateral naris occlusion, to see if we could prevent IgSF8 down-regulation usually seen in adult animals. Sensory deprivation has been demonstrated to arrest mitral cell development in the initial stages of glomerular development, as spontaneous activity is insufficient to drive the morphological development or functional maturation of the glomerular circuit (Maher et al., 2009). Naris occlusion was deemed successful when 1) the OB ipslateral to the occluded nares was reduced in size compared to the contralateral OB (Figure not shown) and 2) when tyrosine hydroxylase expression was greatly reduced in the OB ipsilateral to the occluded nares (Figure 9B, B_1) compared to the contralateral OB (Figure 9A-A_1). Two months after occlusion IgSF8 was still expressed in glomeruli ipslateral to the occluded nares (Figure 9B-B_2) while no, or very low, levels were observed in the contralateral OB (Figure A-A_2). It is possible that sensory deprivation could have altered turnover of OSNs in the OE (leading to an increase in immature, GAP43+ OSNs likely expressing IgSF8), however studies examining the effects of naris occlusion on the OE actually report a decrease in proliferating cells (Cummings and Brunjes, 1994; Suh et al., 2006) Therefore these data argue that functional maturation of the glomerular circuit is necessary for the down-regulation of IgSF8 within glomeruli.

3. DISCUSSION

We show IgSF8 is a developmentally-regulated cell adhesion molecule (CAM) present in OSN axons and temporally on terminals during synaptogenesis. Expression is selectively down-regulated in terminals after glomerular maturation. When the functional maturation of the glomerular circuit is arrested with sensory deprivation, IgSF8 expression is maintained in glomeruli. When axons are induced to regenerate and re-establish synapses, IgSF8 is re-expressed in glomeruli. Our data support the hypothesis that IgSF8 facilitates synaptogenesis in the OB.

4.1 IgSF8 protein-protein interactions

IgSF8 is a cell-surface protein belonging to the novel EWI subfamily which contains a characteristic Glu-Trp-Ile (EWI) extracellular motif (Charrin et al., 2001; Clark et al., 2001; Stipp et al., 2001). IgSF8 has several known interacting proteins, which are all tetraspanins (Tspans). It directly binds to CD9, CD81 and CD82 and indirectly to CD151 (Charrin et al., 2001; Clark et al., 2001; Stipp et al., 2001; Zhang et al., 2003). Although Tspans have small extracellular domains, they do not typically serve as cell-surface receptors, instead they function to organize proteins laterally within membranes (Charrin et al., 2009). The molecular networks they form within membranes, termed tetraspanin-enriched microdomains (TEMs), include proteins from several major classes: adhesion molecules, proteins with Ig-domains; ectoenzymes, and intracellular signaling molecules (Andre et al., 2006; Boucheix and Rubinstein, 2001; Charrin et al., 2009; Hemler, 2005; Le Naour et al., 2006; Levy and Shoham, 2005).

Using immunoprecipitation we demonstrate that IgSF8 interacts with CD9 in the OB. Moreover, *in vitro* IgSF8 is found in discrete puncta, both within OSN axons and growth cones. These puncta are CD9+, indicating IgSF8's presence in TEMs. However not all CD9+ TEMs contained IgSF8, which implies that there may be diversity in TEM composition within OSNs. OSNs are known to differentially express a variety of CAMs (e.g. (Cho et al., 2009) which suggests additional CAMs may be associated with TEMs.

In addition to lateral interactions within TEMs, the intracellular domain of IgSF8 can also associate with actin-linking ezrin-radixin-moesin (ERM) proteins. Thus via ERMs, IgSF8 can act as a linker within TEMs, connecting them directly to the actin cytoskeleton (Sala-Valdes et al., 2006). Moreover, this interaction can facilitate signal transduction events via Rho-GTPases, and in carcinoma cell lines is involved in ERM-dependent processes such as cell migration and polarization. To date, there are no reports of ERM proteins in mouse OSNs, but in chick message is detected in developing olfactory epithelia (Richter et al., 2004). It will be interesting to investigate whether IgSF8 in developing OSN axons is also linked to the actin cytoskeleton via ERM proteins.

IgSF8 at synapses—Based on IgSF8 being present in developing synapses we hypothesized that it facilitates synaptic differentiation and maturation. How might IgSF8 regulate synaptogenesis? Synaptogenesis involves several characteristic steps: 1) contact or adhesion between pre- and post-synaptic cells; 2) presynaptic differentiation to recruit synaptic transmission machinery; and 3) post-synaptic differentiation to receive neurotransmitter signals (Chen and Cheng, 2009; Gerrow and El-Husseini, 2006). The exact mechanisms of recruitment of proteins to forming synapses are not fully understood, but adhesion complexes are well recognized in this process (Biederer and Stagi, 2008).

Our data are consistent with a model in which IgSF8 acts as a CAM during synaptogenesis to stabilize contacts between axons and dendrites while molecular components of the synapse are recruited. How IgSF8 mediates synpatogenesis remains to be determined but one likely possibility is via association with integrins in TEMs (Kolesnikova et al., 2004; Stipp et al., 2003). Consistent with this hypothesis, integrins have well established roles in synaptogenesis. For example, in hippocampal neurons, alpha5 integrin signaling regulates the formation of dendritic spines and synapses (Webb et al., 2007). Somewhat surprisingly, integrin subunit expression has not been assessed in developing glomeruli, or OB synapses. However, our preliminary analyses of α-subunit expression in neonatal OB demonstrates that multiple subunits are present (Supp. Fig S2), many of which are known to interact with IgSF8 in TEMs. Another possibility is that, IgSF8 may be located at sites where cells contact, and bind to ligands such as heat shock proteins (Kettner et al., 2007). Heat shock proteins help in maintaining synaptic machinery (Lu et al., 2010) and their expression has

been reported in rat OSNs (Carr et al., 1994). Whether IgSF8 interacts with heat shock proteins during synaptogenesis in OSNs remains to be determined.

Supporting our hypothesis that IgSF8 facilitates the formation of nascent synapses is the re-expression of Igsf8 within the OB when the olfactory system is induced to regenerate *en masse*.. When OSNs are lesioned, the newly regenerated OSNs express IgSF8, in a similar pattern as that seen in embryonic and postnatal OSNs. Therefore IgSF8 can be detected in regernerating glomeruli in the adult lesioned animals. While one interpretation could be that IgSF8 has a role in OSN maturation, it is also possible that IgSF8 may have an active role in synaptogenesis. Indeed, support for this idea comes from looking at the role of TEMs in synaptogenesis. IgSF8 is a known component of TEMs and interacts with tetraspanins. In Drosophila (which have 36 Tspans) motoneuron axons target muscles appropriately (spatially and temporally) when the Tspan *latebloomer* (lbm) is deleted, however synapse formation is delayed (Kopczynski et al., 1996). Subsequent studies where multiple Tspans were mutated amplified the phenotype, yet synapses still eventually formed (Fradkin et al., 2002), suggesting Tspans facilitate synapse formation but are not essential. IgSF8 null mice have not yet been generated, but it will be interesting to examine synaptogenesis in the absence of this CAM to see if similar delays in synapse formation occur.

IgSF8 in axon shafts—In contrast to expression in synaptic terminals, we found IgSF8 expression in axon shafts to be stable, and to not vary developmentally. This suggests that IgSF8 may have a dual function in OSN axons; acting to facilitate synapses formation during glomerulogenesis and having a separate role in the olfactory nerve and nerve layer. The cytoplasmic tail of IgSF8 binds to phosphatidylionisitolphopshates (PIP) and undergoes palmitoylation, both of which contribute to different IgSF8 functions (He at al., 2011). Interaction with PIP is responsible for IgSF8 stability whereas palmitoylation is necessary for association with tetraspanins. IgSF8 may undergo differential protein modifications in axon shaft versus terminal resulting in differential expression level and function. Although we did not see expression patterns change within the ONL over time, this does not mean proteins are not “fluid” within OSN membranes. TEMs move or “patrol” within membranes (Charrin et al., 2009), and upon particular stimulation become confined within discrete regions of the membrane where more stable interactions occur.

TEMs specifically assemble functionally related adhesion molecules. Yáñez-Mó and colleagues (2009) hypothesize that the clustering of TEM components prepares cells for stepwise adhesion, and importantly, that the microdomains they form are heterogeneous in composition, allowing transmembrane proteins with functionally related processes to interconnect within TEMs. Recently it was established that OSN axons expressing different classes of odor receptors segregate within the olfactory nerve (Bozza et al., 2009) and that during development OSNs sort in the nerve prior to reaching the OB (Imai et al., 2009). It is an attractive hypothesis that IgSF8 containing TEMs in axon shafts facilitate clustering of adhesion molecules in OSN membranes that allow sorting *en route* to glomerular targets. Consistent with this idea, we have detected other TEM components in developing OSNs, including ADAM10 (Andre et al., 2006) (Supp. Figure S2) and MMP14 (Kolesnikova et al., 2009; Yanez-Mo et al., 2008) (Dinglasan, Ray and Treloar, data not shown). In neuronal cell lines, CD9 directly interacts with L1 (Schmidt et al., 1996), which is expressed in developing OSNs (Miragall et al., 1989). It will be interesting to determine whether other CAMs interact with Tspans in OSNs, and whether sorting of axons is TEM dependent.

In summary, we demonstrate that IgSF8 is present in developing OSN synapses, and that it interacts with Tspan CD9. Based on known interactions of IgSF8 and CD9 (elsewhere in the CNS and in carcinoma and immune cells) it is likely that IgSF8 interacts with other CAMs in OSN axons, perhaps regulating maturation and synaptogenesis.

Supplementary Material

Refer to Web version on PubMed Central for supplementary material.

Acknowledgments

This work was supported by DC007600 to HBT. The authors express their thanks to Alexandra Miller, Christine Kaliszewski, Lu Anne Dinglasan, Mike Akins, Diego Rodriguez Gil, Lorena Rela and Dolores Montoya for technical help, Haig Keshishian for helpful discussion, and Janice Mitchell for administrative support

4. REFERENCES

Agarwala KL, Ganesh S, Suzuki T, Akagi T, Kaneko K, Amano K, Tsutsumi Y, Yamaguchi K, Hashikawa T, Yamakawa K. Dscam is associated with axonal and dendritic features of neuronal cells. Journal of neuroscience research. 2001; 66:337–346. [PubMed: 11746351]

Akins MR, Benson DL, Greer CA. Cadherin expression in the developing mouse olfactory system. J Comp Neurol. 2007; 501:483–497. [PubMed: 17278136]

Akins MR, Greer CA. Axon behavior in the olfactory nerve reflects the involvement of catenin-cadherin mediated adhesion. J Comp Neurol. 2006; 499:979–989. [PubMed: 17072833]

Andre M, Le Caer JP, Greco C, Planchon S, El Nemer W, Boucheix C, Rubinstein E, Chamot-Rooke J, Le Naour F. Proteomic analysis of the tetraspanin web using LC-ESI-MS/MS and MALDI-FTICR-MS. Proteomics. 2006; 6:1437–1449. [PubMed: 16404722]

Astic L, Pellier-Monnin V, Saucier D, Charrier C, Mehlen P. Expression of netrin-1 and netrin-1 receptor, DCC, in the rat olfactory nerve pathway during development and axonal regeneration. Neuroscience. 2002; 109:643–656. [PubMed: 11927147]

Biederer T, Stagi M. Signaling by synaptogenic molecules. Curr Opin Neurobiol. 2008; 18:261–269. [PubMed: 18725297]

Bonkobara M, Das A, Takao J, Cruz PD, Ariizumi K. Identification of novel genes for secreted and membrane-anchored proteins in human keratinocytes. Br J Dermatol. 2003; 148:654–664. [PubMed: 12752121]

Booker-Dwyer T, Hirsh S, Zhao H. A unique cell population in the mouse olfactory bulb displays nuclear beta-catenin signaling during development and olfactory sensory neuron regeneration. Dev Neurobiol. 2008; 68:859–869. [PubMed: 18327767]

Boucheix C, Rubinstein E. Tetraspanins. Cell Mol Life Sci. 2001; 58:1189–1205. [PubMed: 11577978]

Bozza T, Vassalli A, Fuss S, Zhang JJ, Weiland B, Pacifico R, Feinstein P, Mombaerts P. Mapping of class I and class II odorant receptors to glomerular domains by two distinct types of olfactory sensory neurons in the mouse. Neuron. 2009; 61:220–233. [PubMed: 19186165]

Carr VM, Murphy SP, Morimoto RI, Farbman AI. Small subclass of rat olfactory neurons with specific bulbar projections is reactive with monoclonal antibodies to the HSP70 heat shock protein. The Journal of comparative neurology. 1994; 348:150–160. [PubMed: 7814683]

Charrin S, Le Naour F, Labas V, Billard M, Le Caer JP, Emile JF, Petit MA, Boucheix C, Rubinstein E. EWI-2 is a new component of the tetraspanin web in hepatocytes and lymphoid cells. The Biochemical journal. 2003; 373:409–421. [PubMed: 12708969]

Charrin S, Le Naour F, Oualid M, Billard M, Faure G, Hanash SM, Boucheix C, Rubinstein E. The major CD9 and CD81 molecular partner. Identification and characterization of the complexes. J Biol Chem. 2001; 276:14329–14337. [PubMed: 11278880]

Charrin S, le Naour F, Silvie O, Milhiet PE, Boucheix C, Rubinstein E. Lateral organization of membrane proteins: tetraspanins spin their web. The Biochemical journal. 2009; 420:133–154. [PubMed: 19426143]

Chen SY, Cheng HJ. Functions of axon guidance molecules in synapse formation. Curr Opin Neurobiol. 2009; 19:471–478. [PubMed: 19828311]

Cho JH, Lepine M, Andrews W, Parnavelas J, Cloutier JF. Requirement for Slit-1 and Robo-2 in zonal segregation of olfactory sensory neuron axons in the main olfactory bulb. J Neurosci. 2007; 27:9094–9104. [PubMed: 17715346]

Cho JH, Prince JE, Cloutier JF. Axon guidance events in the wiring of the mammalian olfactory system. Mol Neurobiol. 2009; 39:1–9. [PubMed: 19048417]

Clark KL, Zeng Z, Langford AL, Bowen SM, Todd SC. PGRL is a major CD81-associated protein on lymphocytes and distinguishes a new family of cell surface proteins. J Immunol. 2001; 167:5115–5121. [PubMed: 11673522]

Cummings DM, Brunjes PC. Changes in cell proliferation in the developing olfactory epithelium following neonatal unilateral naris occlusion. Experimental neurology. 1994; 128:124–128. [PubMed: 8070515]

Dunkley PR, Jarvie PE, Robinson PJ. A rapid Percoll gradient procedure for preparation of synaptosomes. Nat Protoc. 2008; 3:1718–1728. [PubMed: 18927557]

Fogel AI, Akins MR, Krupp AJ, Stagi M, Stein V, Biederer T. SynCAMs organize synapses through heterophilic adhesion. J Neurosci. 2007; 27:12516–12530. [PubMed: 18003830]

Fradkin LG, Kamphorst JT, DiAntonio A, Goodman CS, Noordermeer JN. Genomewide analysis of the Drosophila tetraspanins reveals a subset with similar function in the formation of the embryonic synapse. Proceedings of the National Academy of Sciences of the United States of America. 2002; 99:13663–13668. [PubMed: 12370414]

Gabellec MM, Panzanelli P, Sassoe-Pognetto M, Lledo PM. Synapse-specific localization of vesicular glutamate transporters in the rat olfactory bulb. Eur J Neurosci. 2007; 25:1373–1383. [PubMed: 17425564]

Gerrow K, El-Husseini A. Cell adhesion molecules at the synapse. Front Biosci. 2006; 11:2400–2419. [PubMed: 16720322]

Glazar AI, Evans JP. Immunoglobulin superfamily member IgSF8 (EWI-2) and CD9 in fertilisation: evidence of distinct functions for CD9 and a CD9-associated protein in mammalian sperm-egg interaction. Reprod Fertil Dev. 2009; 21:293–303. [PubMed: 19210920]

Gomez C, Brinon JG, Orio L, Colado MI, Lawrence AJ, Zhou FC, Vidal M, Barbado MV, Alonso JR. Changes in the serotonergic system in the main olfactory bulb of rats unilaterally deprived from birth to adulthood. Journal of neurochemistry. 2007; 100:924–938. [PubMed: 17266734]

Hemler ME. Tetraspanin functions and associated microdomains. Nat Rev Mol Cell Biol. 2005; 6:801–811. [PubMed: 16314869]

Imai T, Yamazaki T, Kobayakawa R, Kobayakawa K, Abe T, Suzuki M, Sakano H. Pre-target axon sorting establishes the neural map topography. Science. 2009; 325:585–590. [PubMed: 19589963]

Kelic S, Levy S, Suarez C, Weinstein DE. CD81 regulates neuron-induced astrocyte cell-cycle exit. Mol Cell Neurosci. 2001; 17:551–560. [PubMed: 11273649]

Kettner S, Kalthoff F, Graf P, Priller E, Kricek F, Lindley I, Schweighoffer T. EWI-2/CD316 is an inducible receptor of HSPA8 on human dendritic cells. Mol Cell Biol. 2007; 27:7718–7726. [PubMed: 17785435]

Kim H, Greer CA. The emergence of compartmental organization in olfactory bulb glomeruli during postnatal development. J Comp Neurol. 2000; 422:297–311. [PubMed: 10842233]

Kolesnikova TV, Kazarov AR, Lemieux ME, Lafleur MA, Kesari S, Kung AL, Hemler ME. Glioblastoma inhibition by cell surface immunoglobulin protein EWI-2, in vitro and in vivo. Neoplasia. 2009; 11:77–86. 74p following 86. [PubMed: 19107234]

Kolesnikova TV, Stipp CS, Rao RM, Lane WS, Luscinskas FW, Hemler ME. EWI-2 modulates lymphocyte integrin alpha4beta1 functions. Blood. 2004; 103:3013–3019. [PubMed: 15070678]

Kopczynski CC, Davis GW, Goodman CS. A neural tetraspanin, encoded by late bloomer, that facilitates synapse formation. Science (New York, N.Y. 1996; 271:1867–1870.

Le Naour F, Andre M, Greco C, Billard M, Sordat B, Emile JF, Lanza F, Boucheix C, Rubinstein E. Profiling of the tetraspanin web of human colon cancer cells. Mol Cell Proteomics. 2006; 5:845–857. [PubMed: 16467180]

Le Naour F, Rubinstein E, Jasmin C, Prenant M, Boucheix C. Severely reduced female fertility in CD9-deficient mice. Science. 2000; 287:319–321. [PubMed: 10634790]

Levy S, Shoham T. The tetraspanin web modulates immune-signalling complexes. Nat Rev Immunol. 2005; 5:136–148. [PubMed: 15688041]

Maher BJ, McGinley MJ, Westbrook GL. Experience-dependent maturation of the glomerular microcircuit. Proc Natl Acad Sci U S A. 2009; 106:16865–16870. [PubMed: 19805387]

Maness PF, Schachner M. Neural recognition molecules of the immunoglobulin superfamily: signaling transducers of axon guidance and neuronal migration. Nat Neurosci. 2007; 10:19–26. [PubMed: 17189949]

Miragall F, Kadmon G, Schachner M. Expression of L1 and N-CAM cell adhesion molecules during development of the mouse olfactory system. Dev Biol. 1989; 135:272–286. [PubMed: 2776969]

Mombaerts P. Axonal wiring in the mouse olfactory system. Annu Rev Cell Dev Biol. 2006; 22:713–737. [PubMed: 17029582]

Murdoch JN, Doudney K, Gerrelli D, Wortham N, Paternotte C, Stanier P, Copp AJ. Genomic organization and embryonic expression of Igsf8, an immunoglobulin superfamily member implicated in development of the nervous system and organ epithelia. Mol Cell Neurosci. 2003; 22:62–74. [PubMed: 12595239]

Nagao H, Yoshihara Y, Mitsui S, Fujisawa H, Mori K. Two mirror-image sensory maps with domain organization in the mouse main olfactory bulb. Neuroreport. 2000; 11:3023–3027. [PubMed: 11006987]

Nakamura K, Hioki H, Fujiyama F, Kaneko T. Postnatal changes of vesicular glutamate transporter (VGluT)1 and VGluT2 immunoreactivities and their colocalization in the mouse forebrain. J Comp Neurol. 2005; 492:263–288. [PubMed: 16217795]

Plachez C, Richards LJ. Mechanisms of axon guidance in the developing nervous system. Curr Top Dev Biol. 2005; 69:267–346. [PubMed: 16243603]

Richter U, Wittler L, Kessel M. Restricted expression domains of Ezrin in developing epithelia of the chick. Gene Expr Patterns. 2004; 4:199–204. [PubMed: 15161100]

Sakamoto T, Kondo K, Kashio A, Suzukawa K, Yamasoba T. Methimazole-induced cell death in rat olfactory receptor neurons occurs via apoptosis triggered through mitochondrial cytochrome c-mediated caspase-3 activation pathway. Journal of neuroscience research. 2007; 85:548–557. [PubMed: 17171702]

Sala-Valdes M, Ursa A, Charrin S, Rubinstein E, Hemler ME, Sanchez-Madrid F, Yanez-Mo M. EWI-2 and EWI-F link the tetraspanin web to the actin cytoskeleton through their direct association with ezrin-radixin-moesin proteins. J Biol Chem. 2006; 281:19665–19675. [PubMed: 16690612]

Schmidt C, Kunemund V, Wintergerst ES, Schmitz B, Schachner M. CD9 of mouse brain is implicated in neurite outgrowth and cell migration in vitro and is associated with the alpha 6/beta 1 integrin and the neural adhesion molecule L1. Journal of neuroscience research. 1996; 43:12–31. [PubMed: 8838570]

Schwob JE. Neural regeneration and the peripheral olfactory system. The Anatomical record. 2002; 269:33–49. [PubMed: 11891623]

Shay EL, Greer CA, Treloar HB. Dynamic expression patterns of ECM molecules in the developing mouse olfactory pathway. Dev Dyn. 2008; 237:1837–1850. [PubMed: 18570250]

Stipp CS, Hemler ME. Transmembrane-4-superfamily proteins CD151 and CD81 associate with alpha 3 beta 1 integrin, and selectively contribute to alpha 3 beta 1-dependent neurite outgrowth. J Cell Sci. 2000; 113(Pt 11):1871–1882. [PubMed: 10806098]

Stipp CS, Kolesnikova TV, Hemler ME. EWI-2 is a major CD9 and CD81 partner and member of a novel Ig protein subfamily. J Biol Chem. 2001; 276:40545–40554. [PubMed: 11504738]

Stipp CS, Kolesnikova TV, Hemler ME. EWI-2 regulates alpha3beta1 integrin-dependent cell functions on laminin-5. J Cell Biol. 2003; 163:1167–1177. [PubMed: 14662754]

Suh KS, Kim SY, Bae YC, Ronnett GV, Moon C. Effects of unilateral naris occlusion on the olfactory epithelium of adult mice. Neuroreport. 2006; 17:1139–1142. [PubMed: 16837842]

Tachibana I, Hemler ME. Role of transmembrane 4 superfamily (TM4SF) proteins CD9 and CD81 in muscle cell fusion and myotube maintenance. J Cell Biol. 1999; 146:893–904. [PubMed: 10459022]

Treloar H, Tomasiewicz H, Magnuson T, Key B. The central pathway of primary olfactory axons is abnormal in mice lacking the N-CAM-180 isoform. J Neurobiol. 1997; 32:643–658. [PubMed: 9183743]

Treloar HB, Purcell AL, Greer CA. Glomerular formation in the developing rat olfactory bulb. J Comp Neurol. 1999; 413:289–304. [PubMed: 10524340]

Treloar HB, Ray A, Dinglasan LA, Schachner M, Greer CA. Tenascin-C is an inhibitory boundary molecule in the developing olfactory bulb. J Neurosci. 2009; 29:9405–9416. [PubMed: 19641104]

Webb DJ, Zhang H, Majumdar D, Horwitz AF. alpha5 integrin signaling regulates the formation of spines and synapses in hippocampal neurons. J Biol Chem. 2007; 282:6929–6935. [PubMed: 17213186]

Yamada O, Tamura K, Yagihara H, Isotani M, Washizu T, Bonkobara M. Neuronal expression of keratinocyte-associated transmembrane protein-4, KCT-4, in mouse brain and its up-regulation by neurite outgrowth of Neuro-2a cells. Neurosci Lett. 2006; 392:226–230. [PubMed: 16203089]

Yanez-Mo M, Barreiro O, Gonzalo P, Batista A, Megias D, Genis L, Sachs N, Sala-Valdes M, Alonso MA, Montoya MC, Sonnenberg A, Arroyo AG, Sanchez-Madrid F. MT1-MMP collagenolytic activity is regulated through association with tetraspanin CD151 in primary endothelial cells. Blood. 2008; 112:3217–3226. [PubMed: 18663148]

Yanez-Mo M, Barreiro O, Gordon-Alonso M, Sala-Valdes M, Sanchez-Madrid F. Tetraspanin-enriched microdomains: a functional unit in cell plasma membranes. Trends Cell Biol. 2009; 19:434–446. [PubMed: 19709882]

Yoshihara Y, Kawasaki M, Tamada A, Fujita H, Hayashi H, Kagamiyama H, Mori K. OCAM: A new member of the neural cell adhesion molecule family related to zone-to-zone projection of olfactory and vomeronasal axons. J Neurosci. 1997; 17:5830–5842. [PubMed: 9221781]

Zhang XA, Lane WS, Charrin S, Rubinstein E, Liu L. EWI2/PGRL associates with the metastasis suppressor KAI1/CD82 and inhibits the migration of prostate cancer cells. Cancer Res. 2003; 63:2665–2674. [PubMed: 12750295]

Zoller M. Tetraspanins: push and pull in suppressing and promoting metastasis. Nat Rev Cancer. 2009; 9:40–55. [PubMed: 19078974]

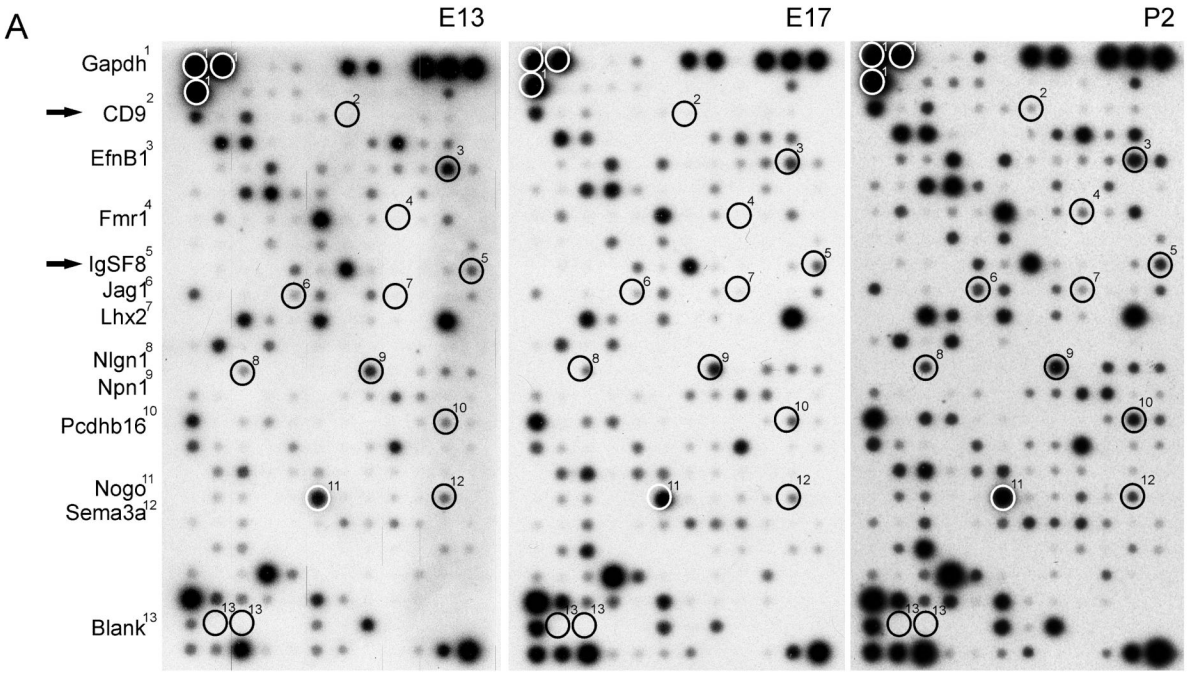

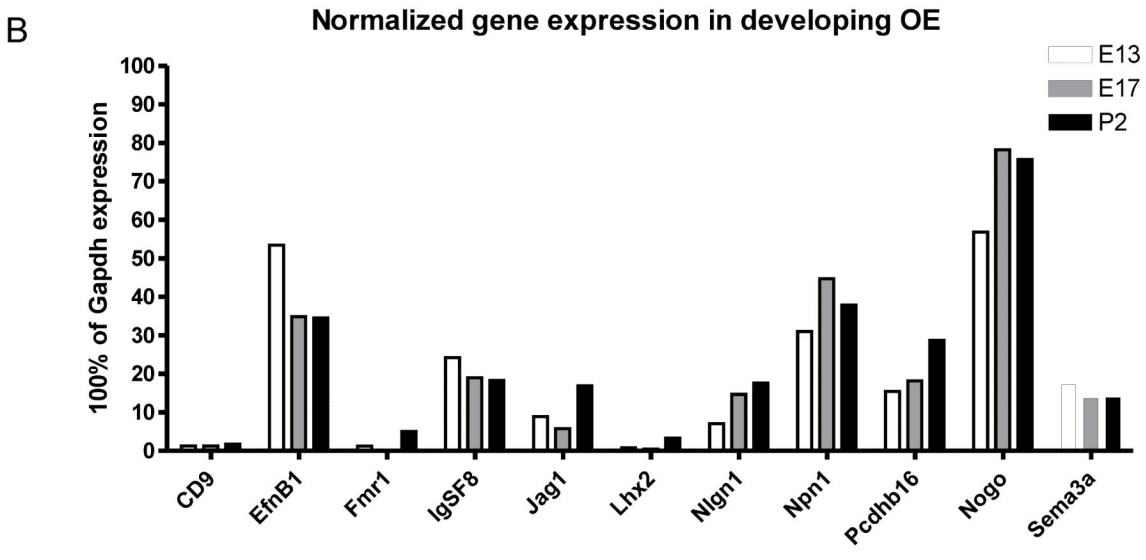

Figure 1.

Gene expression analyses from three different developmental ages (E13, E17 and P2) in the OE **(A)** using Oligo GE Arrays. (A) A selection of candidate developmentally regulated genes (IgSF8, Jag1 and Pcdhb16) as well as some known developmentally regulated genes (Fmr1, Lhx2, Npn1, Nlgn1 and Nogo) were identified in the OE from the Oligo GE array. (B) Relative expression of the identified genes across three developmental ages normalized to GAPDH gene expression from representative arrays. Spot intensity of genes expressed in the OE was normalized to spot intensity of GAPDH gene.

Abbreviations: IgSF8: Immunoglobulin superfamily, member 8; Jag1: Jagged1; Pcdhb 16: Protocadherin beta 16; Fmr1: Fragile X mental retardation syndrome 1 homolog; Lhx2: LIM homeobox protein 2; Npn1: Neuropilin1; Nlgn1: Neuroligin1) .

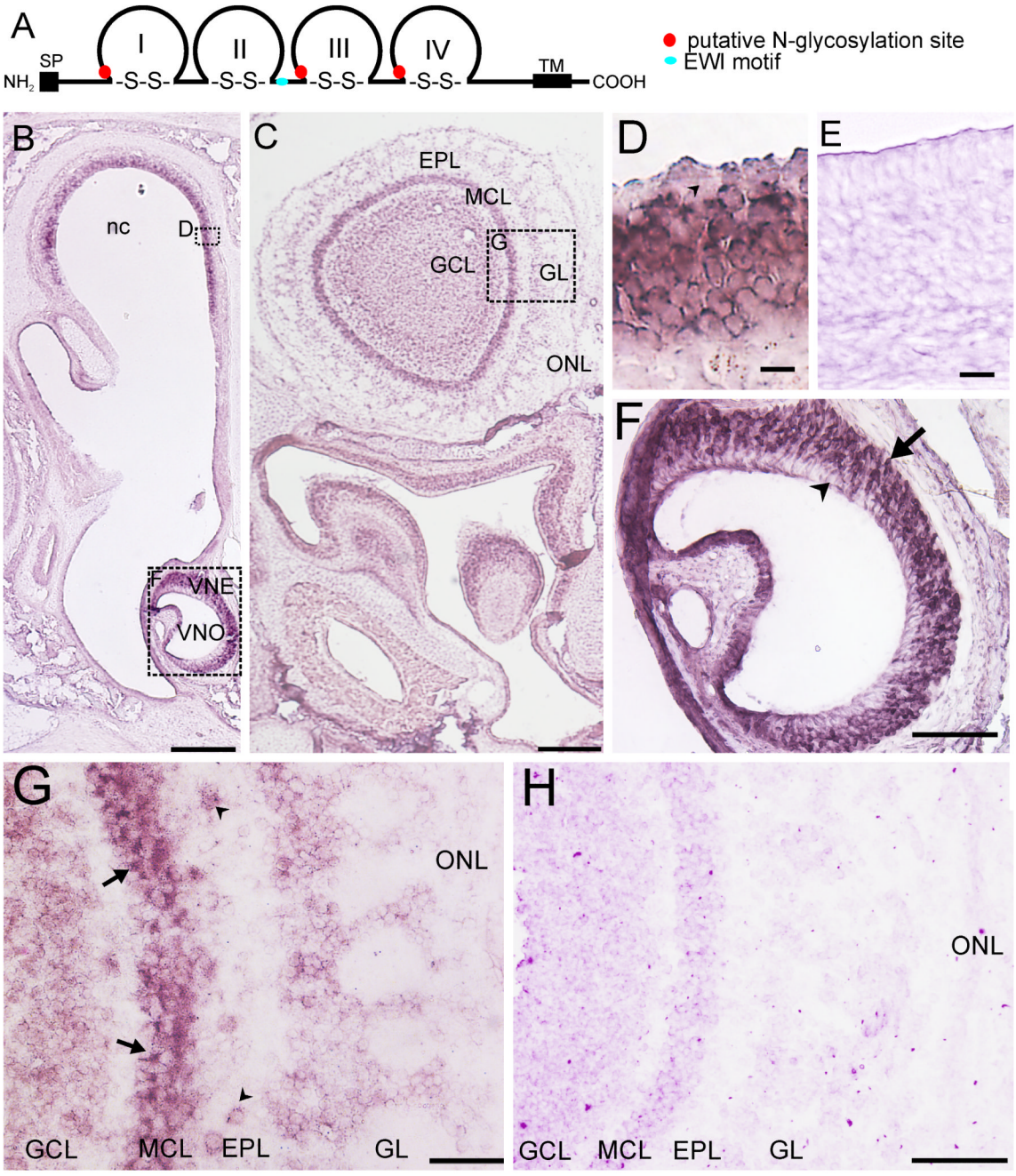

Figure 2.

In situ hybridization (ISH) of IgSF8 in P2 olfactory system. **(A)** A schematic diagram of IgSF8 showing four Ig domains, a transmembrane (TM) region and a short intracellular region. A signal peptide (SP) is present at the amino terminus and each Ig domain consists of a disulfide bond (S-S). Three putative N-glycosylation sites and the EWI motif, which lies outside the second Ig domain, are represented as red and blue circles respectively. **(B)** Coronal section through the rostral nasal cavity (nc). ISH signal is detected in the main olfactory epithelium (OE) and vomeronasal epithelium (VNE). **(C)** Coronal section through the caudal nasal cavity and olfactory bulb (OB). IgSF8 mRNA is found in the OE and within

neuronal populations within the OB. **(D)** A high power micrograph of the main OE (B). Strong signal is detected in the sensory neurons across the extent of the epithelium but the sustentacular cells are devoid of signal (arrowhead). **(E)** No labeling was observed with sense riboprobe in OE. **(F**) A high power micrograph of the vomeronasal organ (VNO) in (B). Strong signal is detected in the vomeronasal sensory neurons (arrow) but the sustentacular cells are devoid of signal (arrowhead). **(G)** A high power micrograph of the OB reveals abundant staining in the mitral cell layer (MCL; arrows) and in some scattered cells (arrowheads) in the external plexiform layer (EPL). Staining is observed in the granule cell layer (GCL) but no staining is observed in the olfactory nerve layer (ONL). **(H)** No labeling was observed with sense riboprobe in OB. GL: glomerular layer. Scale bars, 250μm (B, C); 10 μm (D,E); 100 μm (F); 50 μm (G,H)

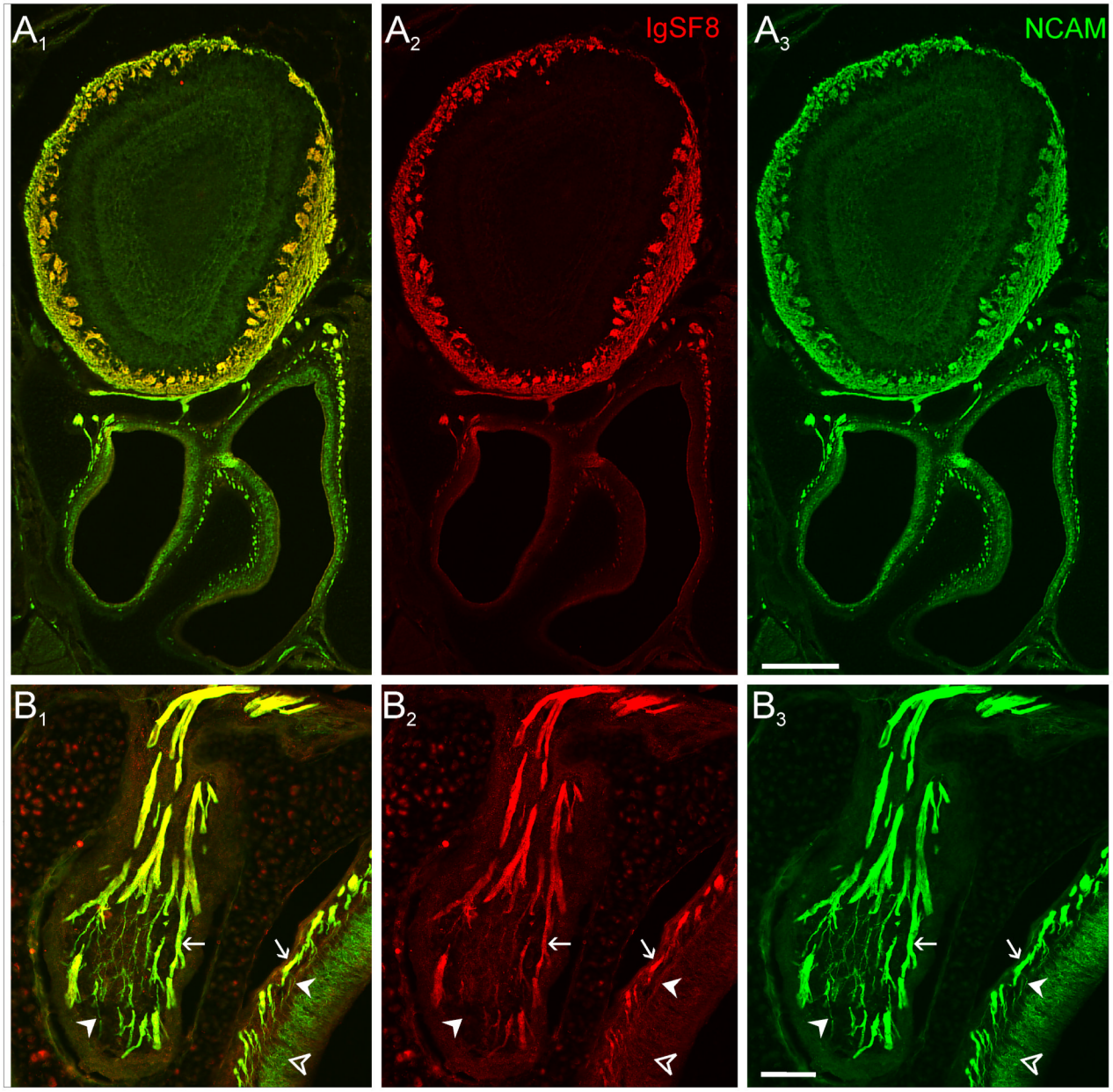

Figure 3.

IgSF8 immunohistochemistry in P2 olfactory system. **(A_1)** Coronal section reveals co-localization of IgSF8 and NCAM in the OB and OE. **(A_2)** IgSF8 expression is similar to **(A_3)** NCAM expression in the OB. Although a higher magnification of OE reveals a differential expression of IgSF8 and NCAM in the axon bundles. **(B_1)** A merged image of IgSF8 and NCAM in the OE. **(B_2)** IgSF8 is expressed only in thicker axon bundles (arrows) and not in finer axon processes (closed arrow heads) or in the cell body (open arrowhead). **(B_3)** NCAM is expressed in the soma of OSNs (open arrow head) as well as in fine (closed arrowheads) and thick axon bundles (arrows). Scale bars, 100μm (A_1-A_3); 500μm (B_1-B_3).

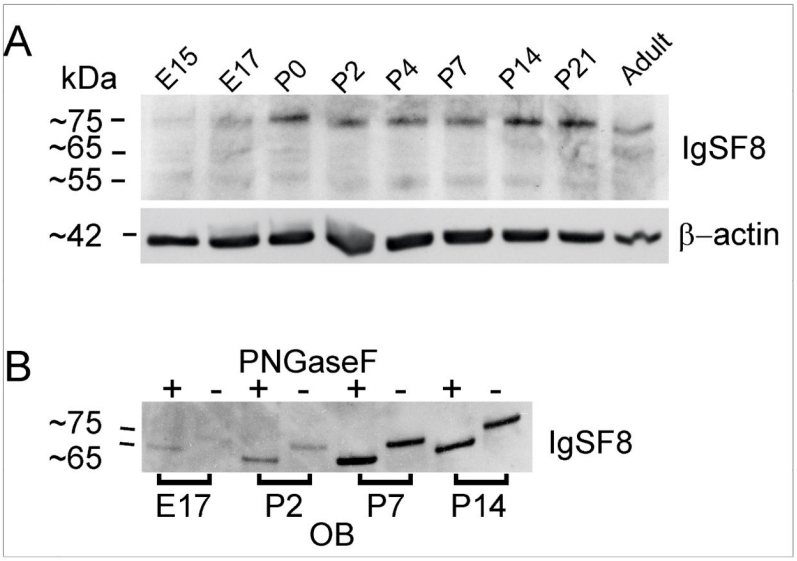

Figure 4.

Developmental expression profile of IgSF8 in the OB. **(A)** OB protein from different ages (E15-Adult) was loaded on a gel and immunoblotted with IgSF8. Three bands of molecular weight ~75kDa, 65kDa and 55kDa are observed. β-actin serves as a loading control. Glycosylation analyses of IgSF8 protein. **(B)** OB lysates digested with PNGaseF are reduced by 10kDa in size compared to control OB lysates.

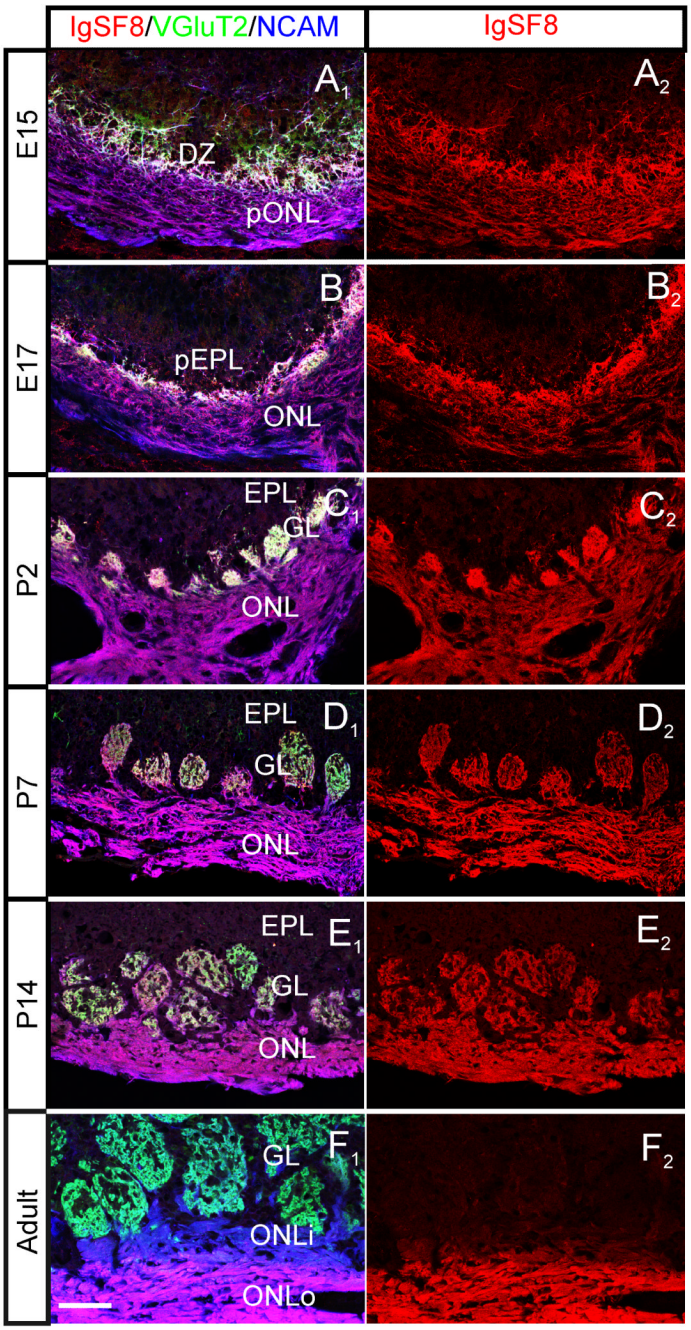

Figure 5.

IgSF8 expression in the developing OSN synapses. **(A1-F1)** Images of a coronal OB section from the ages E15, E17, P2, P7, P14, Adult, triple labeled with IgSF8, VGluT2 and NCAM. VGluT2 is a presynaptic marker of OSNs, and is expressed in the developing glomeruli. NCAM labeling reveals the developmental events during the formation of OB. IgSF8 expression progresses from the presumptive olfactory nerve layer (pONL) to dendritic zone (DZ) at E15, to fully formed glomeruli at P2. The expression is noticeably reduced in the adult glomerular layer (GL) although expression in the olfactory nerve layer (ONL) is maintained at similar levels during development of the OB. Note the gradual change from white glomeruli at P2 (C1) to cyan glomeruli at Adult (F1). IgSF8 expression in the adult

ONL is compartmentalized: it is downregulated in the inner ONL (ONLi) in comparison to the outer ONL (ONLo) as clearly revealed in the triple-labeled image F1. No expression is observed in the presumptive external plexiform layer (pEPL) or in the external plexiform layer (EPL). **(A2-F2)** Corresponding OB images showing IgSF8 immunoreactivity alone. Scale bar = 25μm.

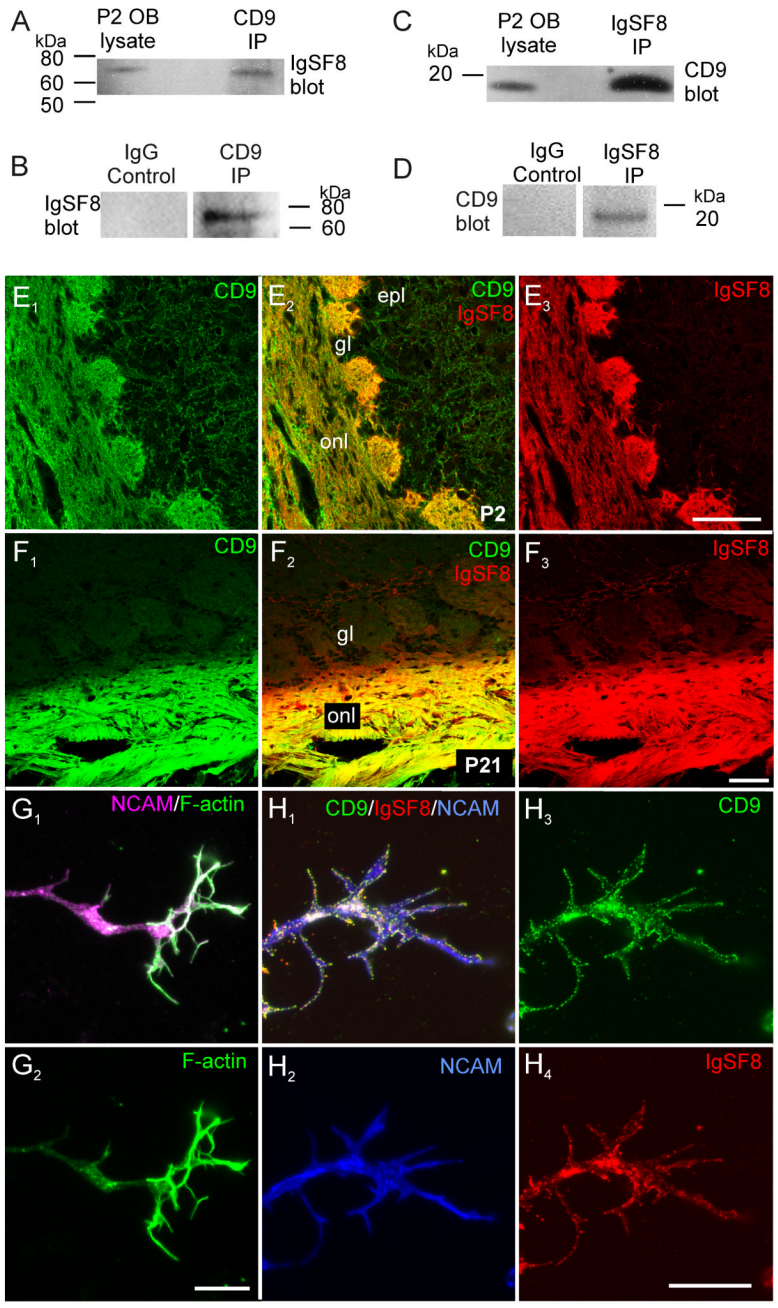

Figure 6.

IgSF8 and CD9 interact in the OB. **(A)** P2 OB homogenized in Brij97 was immunoprecipitated (IP) with CD9 antibody The OB lysate and IP sample were run on a denaturing gel and immunoblotted with IgSF8 antibody. An IgSF8 band of ~75kDa was detected both in the OB lysate and the IP sample. **(B)** OB lysate immunoprecipitated with rat IgG served as a control. No IgSF8 band was detected in this IP sample **(C)** Similarly, a CD9 band of ~19kDa was detected in the OB sample immunoprecipitated with IgSF8. **(D)** No CD9 band was detected in OB sample immunoprecipitated with control goat IgG. **(E_1-E_3)** Co-localization of IgSF8 and CD9 in the glomerular layer (GL) and olfactory nerve layer

(ONL). Signal in the EPL is not above background when compared to control slides. Putative TEM domains in cultured olfactory sensory neurons. **(F1-F3)** At P21, both IgSF8 and CD9 have significantly lower expression in glomeruli compared to the ONL. **(G_1-G_2)** A cultured NCAM+ OSN axon (magenta) showing F-actin (green) enrichment within its growth cone. **(H_1-H_4)** IgSF8 (red) and CD9 (green) expression in cultured NCAM+ OSNs. IgSF8 **(H_4)** and CD9 **(H_3)** form discrete puncta within the membrane of OSN neurites and growth cones, suggestive of these proteins interacting within TEMs. Not all CD9+ puncta (green) are IgSF8+ (red) suggesting molecular diversity of TEMs within OSNs. Scale bars, 50μm (E_1-E_3); 25μm (F_1-F_3)10μm (G_1-H_4)

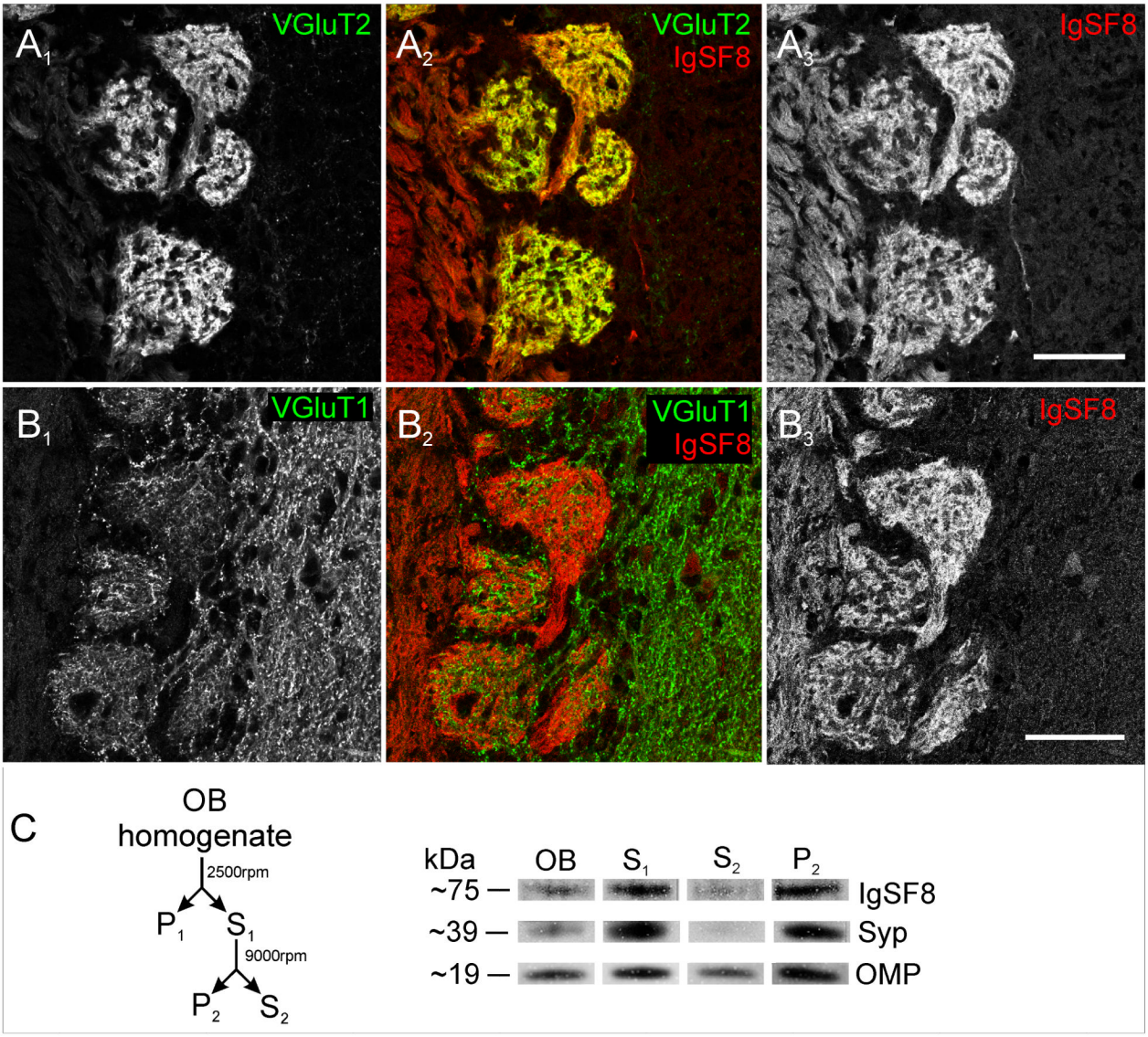

Figure 7.

IgSF8 is enriched in axodendritic synapses. **(A_1-A_3)** VGluT2 is expressed in OSN axon nerve terminals. (A_1) Note the absence of VGluT2 staining in the ONL and EPL. IgSF8 co-localizes with VGluT2 in the glomeruli confirming its presence in OSN axon terminals. **(B_1-B_3)** IgSF8 is not present in the dendrodendritic synapses. VGluT1 expression is abundant in the EPL but no co-localization is observed with IgSF8 in the OB. **(C)** A flowchart indicating the OB tissue fractionation protocol used to obtain a crude synaptosomal fraction (P_2). IgSF8 protein is present in the OB lysate and the postnuclear supernatant (S_1), but further processing of S_1 reveals that the protein is enriched in P_2 versus the synaptosomal supernatant (S_2). OMP serves as a control for OSN terminals and synaptophysin serves as a control for synapse-enriched proteins. Scale bar =50μm.

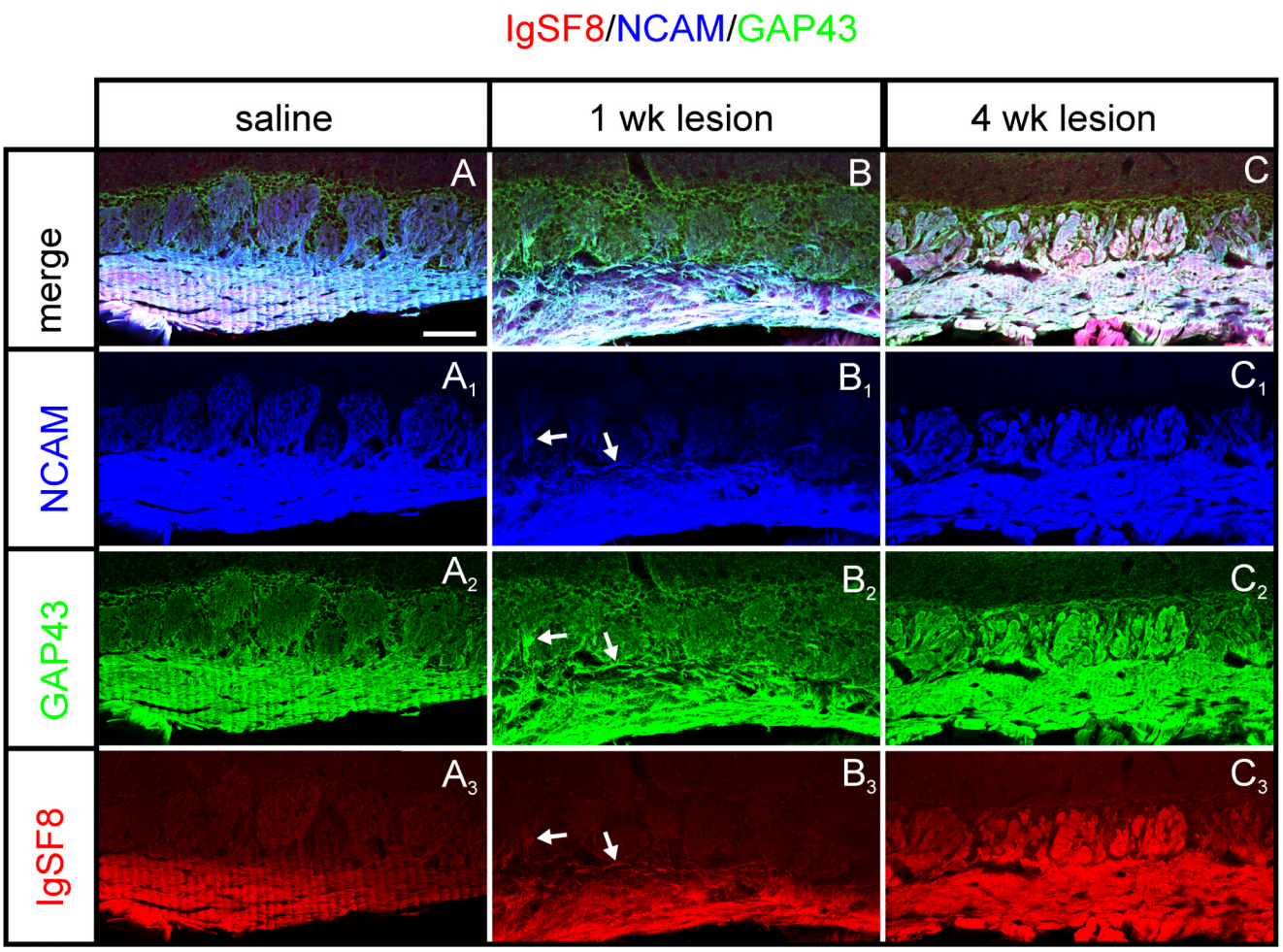

Figure 8.

IgSF8 is upregulated in regenerating OSN axons. Mice injected with the olfactotoxin methimazole were sacrificed one and four weeks after injection. **(A-A_3)** A triple-labeled coronal section from a control (saline injected) mouse reveals strong NCAM and GAP43 expression in the OSNs. IgSF8 expression is strong in the ONL but faint in the adult glomeruli. **(B-B_3)** One week after lesion, OSN axons have not fully regenerated as evident from faint NCAM and GAP43 staining. Few OSN axons which are beginning to regenerate and innervate the glomeruli are triple labeled with IgSF8, NCAM and GAP43 (arrows). **(C-C_3)** Four weeks after lesion, the NCAM and GAP43 expression has been rescued in OSN axons followed by a robust increase of IgSF8 in glomeruli. Scale bar = 100μm.

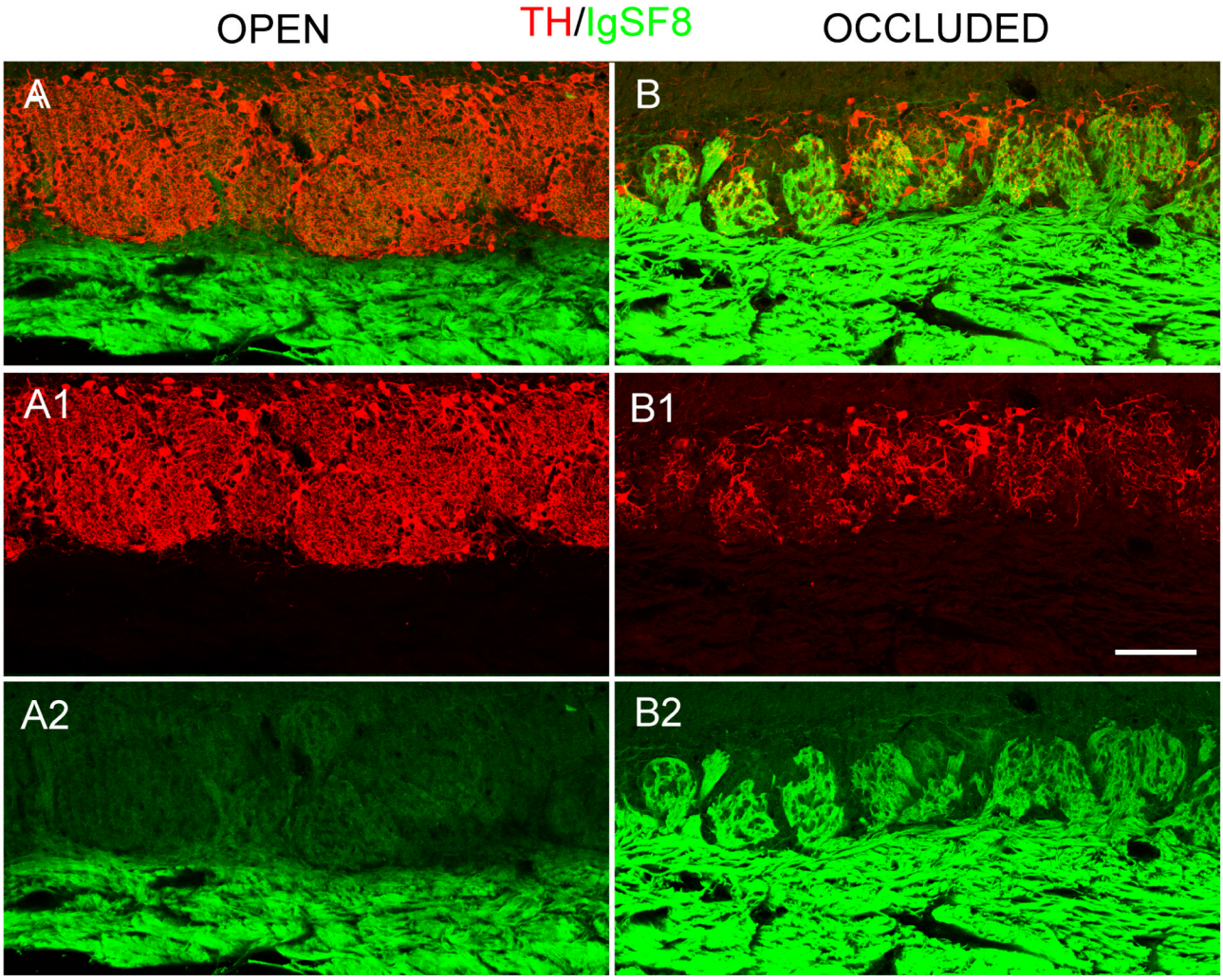

Figure 9.
IgSF8 expression is activity-dependent. (A-A2, B-B2) A high power micrograph of the glomerular layer (GL) of an occluded OB and the contralateral OB. (B-B1) The occluded OB has low levels of TH staining in the GL. The efficiency of occlusion is revealed by low levels of TH staining in the GL of the occluded OB. (A2-B2) GL reveals strong IgSF8 staining in the occluded OB versus the control OB. Scale bar =100μm.

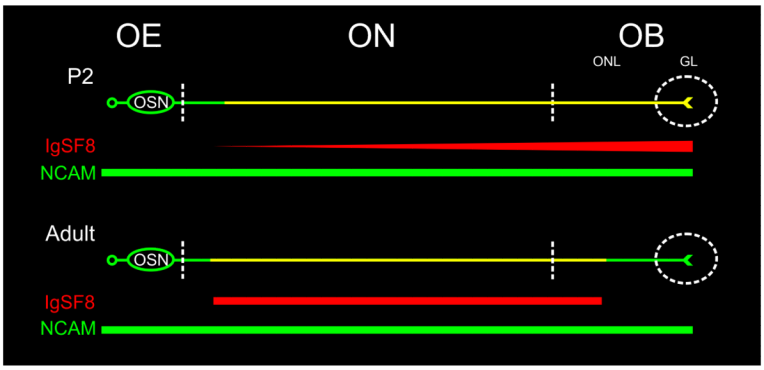

Diagram 1.

Expression of IgSF8 in a P2 and adult OSN. NCAM is expressed along the entire length of a P2 and adult OSN. The soma is devoid of IgSF8 and the expression is confined to the distal part and the terminal of a P2 OSN axon. Co-localization of NCAM and IgSF8 is represented in yellow. IgSF8 expression is downregulated in the adult OSN axon terminal and is confined to the distal portion.